Benzene sensing by Quartz Enhanced Photoacoustic Spectroscopy at 14.85 μm

Diba Ayache, Wioletta Trzpil, Roman Rousseau, Kumar Kinjalk, Roland Teissier, Alexei Baranov, Michael Bahriz, Aurore Vicet

Research Article | Vol. 30, No. 4 / 14 Feb 2022 / Optics Express 5531
Optics EXPRESS

Benzene sensing by Quartz Enhanced Photoacoustic Spectroscopy at 14.85 µm

DIBA AYACHE, WIOLETTA TRZPIL, ROMAN ROUSSEAU, KUMAR KINJALK, ROLAND TEISSIER, ALEXEI N. BARANOV, MICHAEL BAHRIZ, AND AURORE VICET*

IES, University Montpellier, CNRS, 34090 Montpellier, France
aurore.vicet@umontpellier.fr

Abstract: Benzene is a gas known to be highly pollutant for the environment, for the water and cancerogenic for humans. In this paper, we present a sensor based on Quartz Enhanced Photoacoustic Spectroscopy dedicated to benzene analysis. Exploiting the infrared emission of a 14.85 µm quantum cascade laser, the sensor is working in an off-beam configuration, allowing easy alignment and stable measurements. The technique provides a very good selectivity to the sensor and a limit of detection of 30 ppbv in 1 s, i.e. a normalized noise equivalent absorption of 1.95×10^{-8} W.cm^{-1}.Hz$^{-1/2}$. The achieved performances of the sensor have enabled measurements on several air samples of a gas station showing a non-neglectable risk in case of long exposure.

1. Introduction

Benzene (C_6H_6) can be found in many gasoline mixtures in the transport industry, as well as toluene, ethylbenzene, and xylene which are often together designed as the "BTEX" Volatile Organic Compounds (VOC) family. Benzene can also be found in the petroleum and oil refining industry, chemical manufactures and fuel tanks. The benzene concentration in gasoline vapors can reach 200 mg/m^3 (60 ppmv (parts per million)) [1], while in gas stations, a few meters away from the pumps, the measured benzene concentration in ambient air reaches a value of 30 µg/m^3 (10 ppbv). In these ranges of concentrations, benzene is considered carcinogenic. The World Health Organization mentions that concentrations of airborne benzene can be associated to an excess lifetime risk of leukemia of 10^{-4} for 17 µg/m^3 (5 ppbv (parts per billion)) [2], which means that the risk of new leukemia case is one above a background of 10,000. Therefore, there is a solid need to measure and regulate the benzene emissions and prevent workers and public from its exposition.

One of the oldest technics that has proved its selectivity and sensitivity in the gas detection field is gas chromatography, often coupled with mass spectroscopy. This technic can be used to detect benzene but is hardly compatible with in situ sensing. Photoionization or flame ionization presents more compact setups but also lower sensitivity and selectivity. On another hand, optical sensors can lead to very good performances of selectivity and low limits of detection. Optical sensors have been used with success in the past years for the detection of benzene. Infrared sensors have been exploiting the 3.3 µm range using cavity enhanced spectroscopy [3] or multi-pass sensing by difference frequency generation [4]. The ν14 band at 1023 cm^{-1} was also considered using tunable diode laser spectroscopy [5]. Very recently a quantum cascade laser (QCL) was used at 14.8 µm [6] on a cantilever photoacoustic sensor. Quartz Enhanced Photoacoustic Spectroscopy (QEPAS) has never been employed for benzene sensing yet. We present in this paper a benzene sensor based on an off-beam QEPAS design using a quantum cascade laser to target the 14.8 µm ν4 absorption band of the molecule. This wavelength range is accessible thanks to the progress realized during the last years on quantum cascade lasers. It is also particularly interesting as it is

#447197 https://doi.org/10.1364/OE.447197
Journal © 2022 Received 25 Nov 2021; revised 14 Jan 2022; accepted 16 Jan 2022; published 4 Feb 2022

Optics EXPRESS

immune from carbon dioxide (CO_2) or water (H_2O) interferences. Moreover, we have used this sensor to perform ex-situ measurements on the ambient air extracted in a gas station to evaluate the exposition to benzene during car refueling.

QEPAS sensing relies on photoacoustic spectroscopy using a quartz tuning fork (QTF) as a piezoelectric transducer to convert the mechanical displacement into a readable electrical signal [7]. Small cylindrical tubes (called micro-resonators, mR) are used to confine the generated acoustic wave [8] and increase the overall signal. A major issue with QCL lasers, specifically above 10 µm, can be the highly divergent beam compared to near-infrared lasers. In the conventional on-beam QEPAS configuration, the QCL laser beam would hit the QTF prongs thus creating unwanted signal background due to the photothermal effect, even if it can be used in specific conditions like presented in [9]. One solution is to employ a custom QTF with larger prong spacing [10]. Another solution is the use of the off-beam configuration, which is compatible with the divergence of QCLs [11]. The off-beam configuration was studied theoretically and implemented in detecting various molecular species [8,11–13]. Eventually, the QTF can be embedded in an acoustic resonant cavity [14]. For this work, we present for the first time a QEPAS sensor based on an off-beam design with a quantum cascade laser targeting the 14.8 µm benzene absorption band.

2. Experiment setup

We used a distributed feedback (DFB) laser fabricated by molecular beam epitaxy in the InAs/AlSb material family in Montpellier University [15]. Its side mode suppression ratio reaches 30 dB (Fig. 1.a), which ensures a very good spectral purity suitable for spectroscopy. The laser works in continuous wave regime at temperatures from −10°C to 10°C. Figure 1.a presents an example of the emitted spectra at T= - 10°C and I = 750 mA. Figure 1.b presents the emitted power and voltage versus the injected current. The threshold current value at −10°C is 530 mA, the emitted power reaches 7 mW, and the low frequency tuning rate is - 0.0047 cm^{-1}/mA.

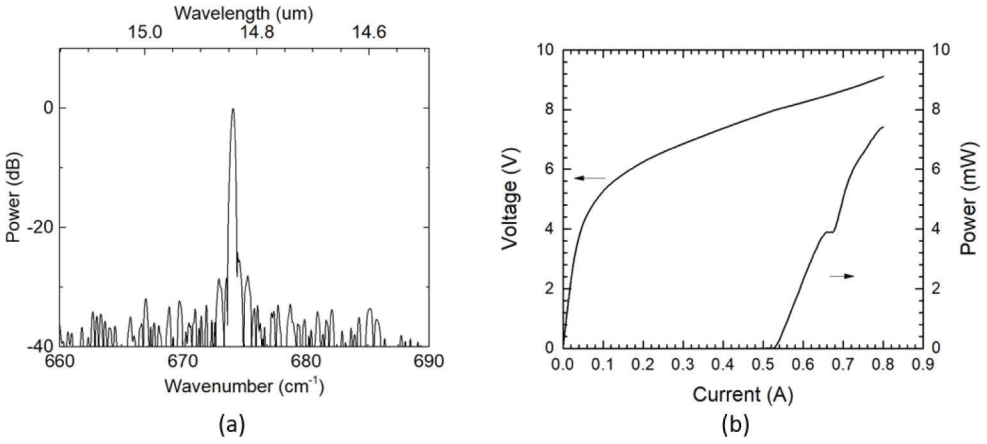

Fig. 1. (a) The emission spectrum of the quantum cascade laser recorded at a temperature of −10°C and injected current of 750 mA. (b) Electrical characterization and emitted power recorded at −10°C. All measurements were done in continuous wave regime. A CO_2 ambient absorption line is detected at 670 mA.

We operated the laser at −10 °C to perform the sensing acquisitions because it was the best condition to reach the benzene absorption line at 773 mA. This line is reported in Fig. 2., at atmospheric pressure. This simulated absorption spectrum is given by a cross-section file of the HITRAN database [16] for a concentration of 1 ppmv and 1 cm path length. The main benzene

Optics EXPRESS

line, located at 673.96 cm^{-1}, is thin with a half width at half maximum of 0.12 cm^{-1}. Ambient CO_2 presents two absorption peaks in the same region. However, they are on both sides of the benzene peak (precisely at 672.86 cm^{-1} and 674.44 cm^{-1} with strengths 1.143×10^{-19} and $1.358\,x10^{-19}$ cm^{-1}/molecules.cm^{-2}, respectively) and should not affect its measurement. We have reported on the same plot the emitted wavelength of the laser for different currents from 600 to 800 mA, in continuous wave regime at −10°C.

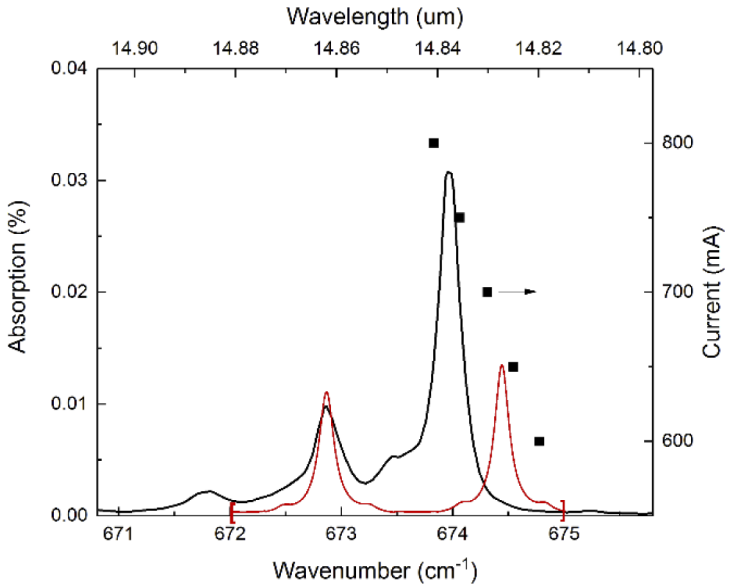

Fig. 2. Black line: Simulation of the absorption spectrum of benzene, central part of v4 branch, for a concentration of 1 ppmv. This spectrum is extracted from the cross-sections spectra of the HITRAN spectroscopic database. Red line: Simulation of the absorption spectrum of CO_2, for a concentration of 10 ppmv. The absorption path length is set to 1 cm. The corresponding emitted wavelengths of the laser are reported in black squares for different injected currents at −10°C.

The sensor setup is presented on Fig. 3. The laser is enclosed in a homemade sub mount with a PT100 temperature sensor and a Peltier cooler, and closed under dry nitrogen to avoid water condensation on the laser chip. A double lens optical setup could be efficient to adjust more accurately the position of the focal point inside the micro-resonator. However, we preferred a single lens mount to preserve a larger part of the optical power of the laser. The strongly divergent emitted beam crosses a KBr (Potassium Bromide) window and is directed to a ZnSe lens L1 of 10 mm focal length. Then, the beam goes through a ZnSe (Zinc Selenide) window into the gas cell containing the spectrophone, composed of a standard commercial quartz tuning fork and an aluminum micro-resonator. The micro-resonator was adapted to the large beam profile of the quantum cascade laser wavelength with a diameter of 0.7 mm for the main hole. The mR length is 6.1 mm [17] and the diameter of the perpendicular coupling hole is 0.5 mm. The QTF position is optimized following [11], as it can be seen in Fig. 3. The quartz tuning fork is accurately characterized and its resonance frequency and quality factor are monitored during the experiments. The observed values are: $f_0 = 32758.4$ Hz and $Q = 3377$.

The measured emitted power of the laser after passing windows and lens(es) was 3 mW. The photodetector was unable to measure the loss caused by the ZnSe window (Transmission for a 5 mm width at 14.9 um = 70%) at the gas cell's entry, as well as the inner diameter of the mR, since the BaF_2 (Barium Fluoride) window at the available gas cell's exit transmits light only

Optics EXPRESS

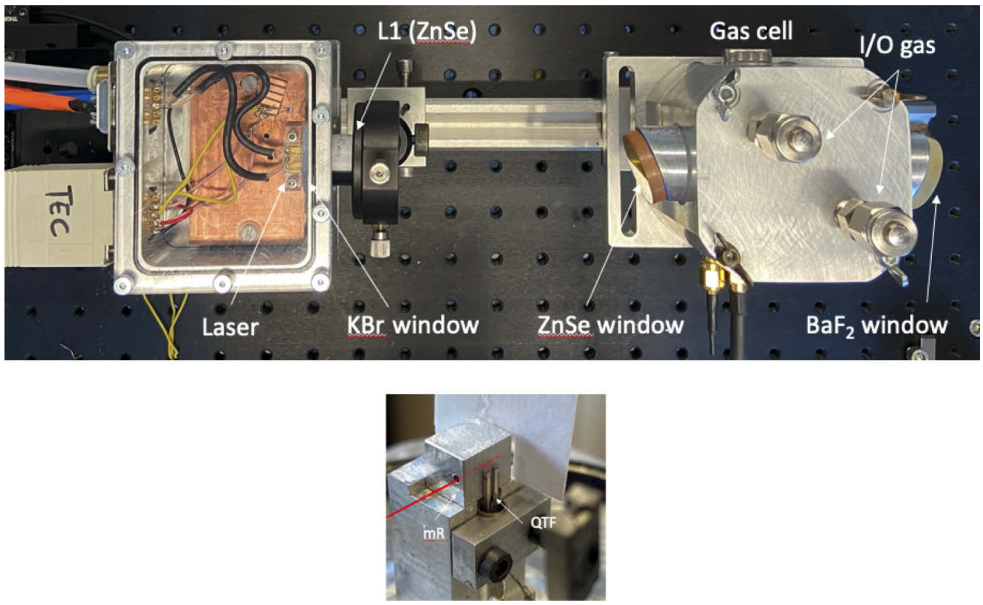

Fig. 3. Optical setup (top picture) and zoom (bottom picture) on the quartz tuning forks (QTF) positioned in front of the micro-resonator (mR). The QTF and mR are located inside the gas cell.

until 10 µm. The power of the laser inside the gas cell was estimated to 2.1 mW by taking into account the loss caused by the ZnSe window.

The laser is driven with a slow current ramp to tune the central emission wavelength, which is additionally modulated with a high frequency sinusoidal current for wavelength modulation. In QEPAS, the high frequency modulation corresponds to a harmonic of the QTF fundamental frequency f_0. In our experiment, the laser was driven in $2f$ ($f = f_0/2$) mode, to perform Wavelength Modulation Spectroscopy (WMS) at the second harmonic.

3. Sensor calibration

The gas mixtures were prepared using a gas mixing system (Alytech GasMix Aiolos II) to provide accurate and controlled dilutions of benzene in dry nitrogen at atmospheric pressure and at a constant flow rate (0.5 L/min). Several dilutions were made to evaluate the signal given by the sensor and its linearity. Figure 4. shows different concentration steps and the corresponding plot of the signal amplitude. The setup exhibits a very good linearity ($R = 0.9994$). The data were extracted from *2f* spectra acquired using a time constant of 200 ms on an EG&G Instruments Model 7220 Dual Phase Lock in Amplifier (LIA). One can see that the signal corresponding to a 100 ppbv of benzene concentration can still be observed above the noise level (1σ).

Water is known to have an effect on the relaxation time of the molecules. For some gases, the amplitude of the observed QEPAS signal is at least two times higher when the gas mixture is humidified [17]. In the case of benzene, the contrary was observed as can be confirmed by [18]. The QEPAS signal measured for a humidified concentration was lower than for a dry concentration. But even if humidity decreases the performances of our sensor, it is necessary to have calibrated curves of the QEPAS signal for wet benzene because, as we aim to work on samples from ambient air, the humidity needs to be considered. For dry benzene measurements, the output of the gas mixing system was directly connected to the gas cell. For wet benzene measurements, the output of the gas mixing system was connected to a homemade bubble bath before going to the gas

Optics EXPRESS

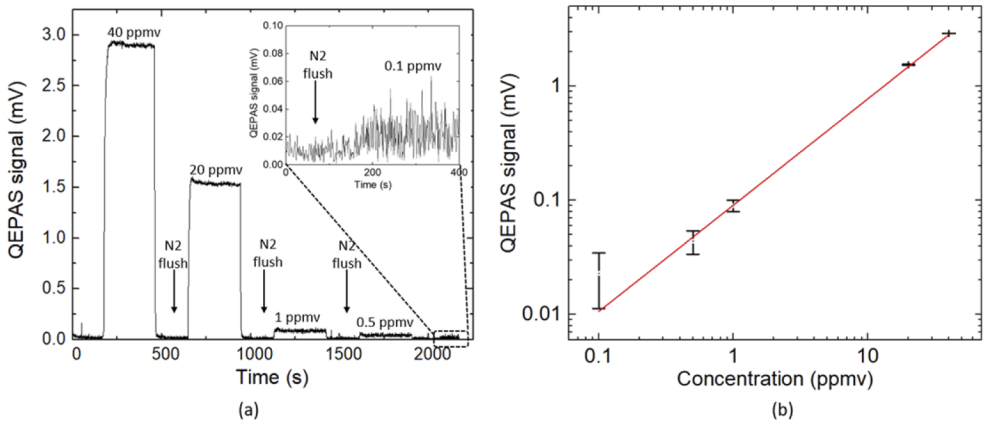

Fig. 4. (a) Amplitude of the QEPAS signal corresponding to several successive injections of calibrated benzene/N_2 mixtures followed by nitrogen flush of the gas cell. (b): the corresponding calibration curve shows a good linearity of the signal with the gas concentration.

cell. The 95% humidity was measured inside the gas cell in this configuration. Using linear interpolation, we estimated the signal for different humidity corresponding to the amount of humidity we measured for each sampling day at the gas station (cf. section 4). The calculated calibration curves are represented in Fig. 5.

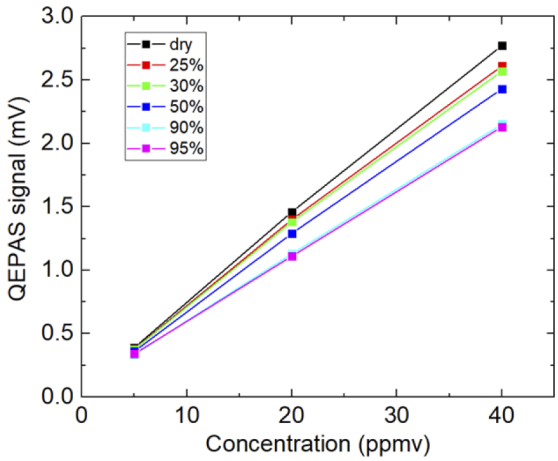

Fig. 5. Magnitude of QEPAS signal calculated for 40, 20 and 5 ppmv of benzene for 25, 30, 50 and 90%RH (relative humidity). A linear interpolation was used to calculate these magnitudes using the signal obtained for calibrated dry and wet (95%RH) benzene concentrations.

To evaluate the detection limit for a given integration time and the real performances of the sensor, we have plotted the Allan-Werle variance (Fig. 6.). For this, we recorded a QEPAS signal of a 5 ppmv calibrated Benzene-N_2 mixture during 30 min. The results showed a limit of detection (1σ) of 30 ppbv in 1 second and it reaches 4 ppbv in 120 s. This corresponds to a NNEA value of $1.95 \times 10–8$ W.cm^{-1}.Hz$^{-1/2}$.

The long-term drift of the sensor appears relatively early (120 s), showing that the measure could be more stabilized, as a small leakage was observed with time.

Optics EXPRESS

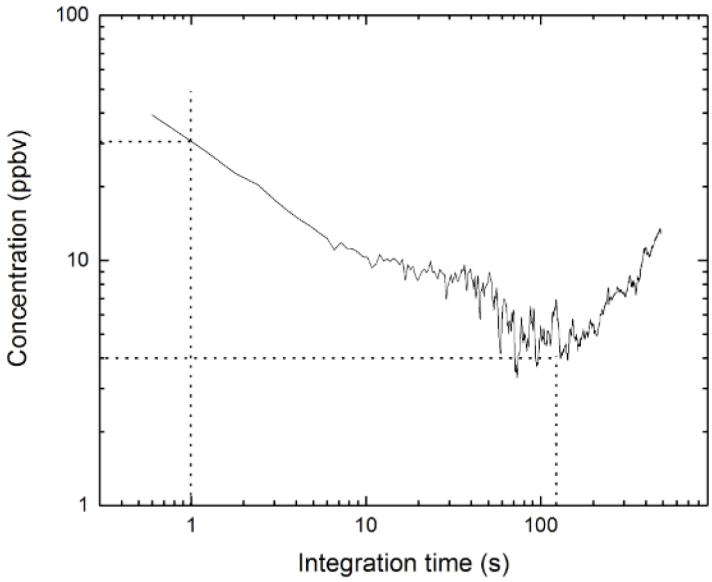

Fig. 6. Allan-Werle deviation measurement of a constant QEPAS signal corresponding to 5 ppmv of Benzene in pure nitrogen. The acquisition time was 30 min and was performed with the laser working under an injected current of 773 mA, with an amplitude modulation of 56 mA and for a given temperature of −10 °C.

4. Gas station measurements

As mentioned before, benzene is present in gasoline and thus, can be measured in the ambient air of a gas station. We have chosen a gas station near the laboratory, where many pumps were available, to evaluate the benzene public exposures. The station is located in a large external place with only a high roof to protect from the rain, but no other walls. The weather conditions are then very important and need to be considered to describe the sampling experimental conditions. In order to monitor the benzene concentration in different places in this gas station, we have performed ex-situ measurements. Air samples were collected in Tedlar bags and the measurement was performed in the laboratory in a short time delay. The sampling was performed during four consecutive days at different places in the gas station. While a person was refilling its car tank (with car windows kept open) the air was collected: a) very close to the gasoline pump, b) 1 meter away from the gas pump, c) 2 meters away from the gas pump. After the refilling, the windows of the car were closed and an air bag was extracted from inside the car, on the passenger seat next to the driver. The main objective of these measurements was to determine if there is a risk of exposition to high concentration of benzene. The Table 1 describes, day by day, the weather conditions (temperature (°C), relative humidity (%RH) and wind velocity (km/h)) and the benzene concentration measured at each position.

In Fig. 7. can be seen the QEPAS signal obtained for samples extracted at the gas station. It is a *2f* signal, showing a well recognizable shape. These samples correspond to days 2 and 3 of measurements. Based on Fig. 5., benzene concentration corresponding to the QEPAS signal was evaluated by taking into account the humidity measured for each day. The CO_2 concentration was evaluated as well, exploiting the side line described in Fig. 2. The CO_2 calibration was realized considering the relative absorption and the relative line strength of the two CO_2 and C_6H_6 lines.

The relative dispersion observed for the different measurements can be explained by the different weather conditions: the wind conditions can lead to local dilutions or turbulences with

Optics EXPRESS

Table 1. Weather Conditions and Benzene Measurements in a Gas Station.

	Day 1		Day 2		Day 3		Day 4	
Temperature (°C)	26		25		24		17	
Relative humidity (%)	90		30		25		50	
Wind velocity (km/h)	17		8		20		25-30	
Benzene measurements (ppmv)	Gas pump	27.3	Gas pump	12.4	Gas pump		Gas pump	4.2
	1m		1m	0.29	1m	2.9	1m	2.3
	2m		2m	1.6	2m		2m	3.3
	Inside car		Inside car		Inside car	1.25	Inside car	9.5

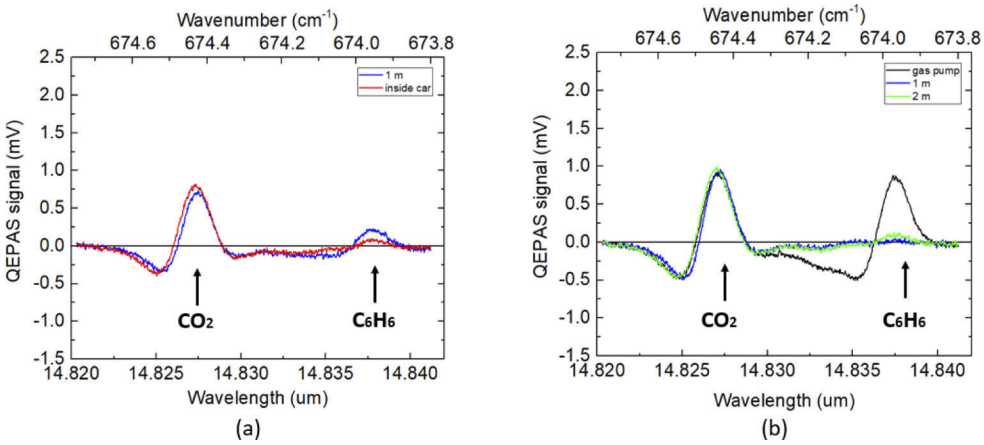

Fig. 7. QEPAS signal measured for gas station samples. (a) represents the signal for day 2 and (b) represents the signal for day 3. The corresponding concentrations are represented in the Table 1. The operating temperature of the laser was set at −10°C. The time constant of the LIA was set to100 ms and the sensitivity to 500 µV.

higher concentrations. The various relative humidity in the ambient air can also lead to some variations up to 10% from 20 to 50%RH.

Nevertheless, one can retain that:

- Concentrations just near the pump are realistic compared to benzene concentration in gasoline vapors [1]. These measured concentrations far exceed the standards defined for regulation. While it can be tolerable for the public for very short exposures, it can have significant consequences on workers that are longer exposed to these high amounts. One can observe that the concentrations decrease quickly with the distance from the pump in agreement with [19], even if local effects can appear with turbulences and wind.

- Surprisingly, we were able to measure benzene concentration inside the car after the refilling. If we consider the weather conditions, these concentrations increase with the wind velocity. We can assume that a “trap effect” appears when refilling with open windows. It would be interesting to monitor the air in the car to estimate how long these concentrations can still be measured.

Optics EXPRESS

- The CO_2 concentration was evaluated to 385 ppmv, a bit lower than actual ambient concentrations, and may be confirmed by specific measurements in a new campaign.

5. Conclusion

This paper presents the first reported results of an off-beam quartz enhanced photoacoustic sensor dedicated to benzene detection, relying on a 14.85 µm quantum cascade laser. The performances of the sensor show a normalized noise equivalent absorption of 1.95×10^{-8} W.cm^{-1}.Hz$^{-1/2}$, corresponding to a limit of detection of 30 ppbv in 1s or 4 ppbv in 120 s. Moreover, by means of ex-situ measurements performed on 4 different days, we have been able to evaluate the benzene concentration in a public gas station: the environment on which the drivers are highly exposed. It is the first reported measurement of this type. As a perspective, we plan to install our sensor for a longer duration in the station and record the benzene concentration during long periods to follow in real time the evolution of benzene emissions. Presented results confirms that this sensor is suitable for measurements and regulation purposes in industries or public applications.

Funding. Agence Nationale de la Recherche (ANR-16-CE04-0012, ANR-11-EQPX-0016); Université de Montpellier (MUSE - 2020 - SENSIR).

Disclosures. The authors declare no conflicts of interest.

Data availability. Data underlying the results presented in this paper are not publicly available at this time but may be obtained from the authors upon reasonable request.

References

1. S. M. Correa, G. Arbilla, M. R. C. Marques, and K. M. P. G. Oliveira, "The impact of BTEX emissions from gas stations into the atmosphere," Atmos. Pollut. Res. **3**(2), 163–169 (2012).
2. WHO, "Exposure To Benzene: a Major Public Health Concern," Prev. Dis. Through Heal. Environ. 3–6 (2019).
3. M. Mhanna, G. Zhang, N. Kunnummal, and A. Farooq, "Cavity-Enhanced Measurements of Benzene for Environmental Monitoring," IEEE Sens. J. **21**(3), 3849–3859 (2021).
4. J. Cousin, W. Chen, D. Bigourd, M. Fourmentin, and S. Kassi, "Telecom-grade fiber laser-based difference-frequency generation and ppb-level detection of benzene vapor in air around 3 µm," Appl. Phys. B **97**(4), 919–929 (2009).
5. J. Waschull, B. Sumpf, Y. Heiner, and H. D. Kronfeldt, "Diode laser spectroscopy in the ν14 band of benzene," Infrared Phys. Technol. **37**(1), 193–198 (1996).
6. J. Karhu, H. Philip, A. Baranov, R. Teissier, and T. Hieta, "Sub-ppb detection of benzene using cantilever-enhanced photoacoustic spectroscopy with a long-wavelength infrared quantum cascade laser," Opt. Lett. **45**(21), 5962 (2020).
7. A. A. Kosterev, Y. A. Bakhirkin, R. F. Curl, and F. K. Tittel, "Quartz-enhanced photoacoustic spectroscopy," Opt. Lett. **27**(21), 1902 (2002).
8. H. Yi, K. Liu, S. Sun, W. Zhang, and X. Gao, "Theoretical analysis of off beam quartz-enhanced photoacoustic spectroscopy sensor," Opt. Commun. **285**(24), 5306–5312 (2012).
9. S. Qiao, Y. Ma, Y. He, P. Patimisco, A. Sampaolo, and V. Spagnolo, "Ppt level carbon monoxide detection based on light-induced thermoelastic spectroscopy exploring custom quartz tuning forks and a mid-infrared QCL," Opt. Express **29**(16), 25100 (2021).
10. P. Patimisco, A. Sampaolo, M. Giglio, S. dello Russo, V. Mackowiak, H. Rossmadl, A. Cable, F. K. Tittel, and V. Spagnolo, "Tuning forks with optimized geometries for quartz-enhanced photoacoustic spectroscopy," Opt. Express **27**(2), 1401 (2019).
11. R. Rousseau, Z. Loghmari, M. Bahriz, K. Chamassi, R. Teissier, A. N. Baranov, and A. Vicet, "Off-beam QEPAS sensor using an 11-µm DFB-QCL with an optimized acoustic resonator," Opt. Express **27**(5), 7435 (2019).
12. K. Liu, H. Yi, A. A. Kosterev, W. Chen, L. Dong, L. Wang, T. Tan, W. Zhang, F. K. Tittel, and X. Gao, "Trace gas detection based on off-beam quartz enhanced photoacoustic spectroscopy: Optimization and performance evaluation," Rev. Sci. Instrum. **81**(10), 103103 (2010).
13. T. Rück, R. Bierl, and F. M. Matysik, "NO2 trace gas monitoring in air using off-beam quartz enhanced photoacoustic spectroscopy (QEPAS) and interference studies towards CO2, H2O and acoustic noise," Sensors and Actuators B: Chemical **255**, 2462–2471 (2018).
14. H. Lv, H. Zheng, Y. Liu, Z. Yang, Q. Wu, H. Lin, B. A. Z. Montano, W. Zhu, J. Yu, J. Yu, R. Kan, Z. Chen, and F. K. Tittel, "Radial-cavity quartz-enhanced photoacoustic spectroscopy," Opt. Lett. **46**(16), 3917–3920 (2021).
15. H. N. Van, Z. Loghmari, H. Philip, M. Bahriz, A. N. Baranov, and R. Teissier, "Long wavelength (λ > 17 µm) distributed feedback quantum cascade lasers operating in a continuous wave at room temperature," Photonics **6**(1), 31 (2019).
16. I. E. Gordon, L. S. Rothman, C. Hill, R. V. Kochanov, Y. Tan, P. F. Bernath, M. Birk, V. Boudon, A. Campargue, K. V. Chance, B. J. Drouin, J. M. Flaud, R. R. Gamache, J. T. Hodges, D. Jacquemart, V. I. Perevalov, A. Perrin, K. P. Shine, M. A. H. Smith, J. Tennyson, G. C. Toon, H. Tran, V. G. Tyuterev, A. Barbe, A. G. Császár, V. M. Devi,

Optics EXPRESS

T. Furtenbacher, J. J. Harrison, J. M. Hartmann, A. Jolly, T. J. Johnson, T. Karman, I. Kleiner, A. A. Kyuberis, J. Loos, O. M. Lyulin, S. T. Massie, S. N. Mikhailenko, N. Moazzen-Ahmadi, H. S. P. Müller, O. V. Naumenko, A. V. Nikitin, O. L. Polyansky, M. Rey, M. Rotger, S. W. Sharpe, K. Sung, E. Starikova, S. A. Tashkun, J. Vander Auwera, G. Wagner, J. Wilzewski, P. Wcisło, S. Yu, and E. J. Zak, "The HITRAN2016 molecular spectroscopic database," J. Quant. Spectrosc. Radiat. Transf. **203**, 3–69 (2017).

17. N. Maurin, R. Rousseau, W. Trzpil, G. Aoust, M. Hayot, J. Mercier, M. Bahriz, F. Gouzi, and A. Vicet, "First clinical evaluation of a quartz enhanced photo-acoustic CO sensor for human breath analysis," Sensors and Actuators B: Chemical **319**, 128247 (2020).
18. J. Karhu and T. Hieta, "Enhancement of photoacoustic spectroscopy with sorption enrichment for ppt-level benzene detection," ChemRxiv (2021).
19. R. Sur, Y. Ding, R. B. Jackson, and R. K. Hanson, "Tunable laser-based detection of benzene using spectrally narrow absorption features," Appl. Phys. B **125**(11), 195 (2019).